11th Asia-Pacific Conference on Combustion,
The University of Sydney, NSW Australia
10th -14th December 2017.

# A Numerical Study of Flame Instability and Cell Dynamics of Opposed Nonpremixed Tubular Flames near Radiation-Induced Extinction Limit

**Hyun Su Bak[1], Chun Sang Yoo[1, 2, *]**

[1]Department of Mechanical Engineering, Ulsan National Institute of Science and Technology

50 UNIST-gil Banyeon-ri Eonyang-eup Ulju-gun, Ulsan, 44919, Republic of Korea

[2]School of Mechanical, Aerospace and Nuclear Engineering, Ulsan National Institute of Science and Technology

50 UNIST-gil Banyeon-ri Eonyang-eup Ulju-gun, Ulsan, 44919, Republic of Korea

## Abstract

The flame instability and cell dynamics of opposed nonpremixed tubular flames near radiation-induced extinction limit are investigated using high fidelity numerical simulations with various initial conditions (IC). When the radiation effect is considered, two different extinction Damköhler numbers (i.e. large radiation-induced extinction Damköhler number, $Da_{E,R}$, and high stretch-induced extinction Damköhler number, $Da_{E,S}$) are obtained by 1-D analysis with different radiative intensity, $I$. Two critical $Da$s, $Da_{C,C}$ and $Da_{C,O}$, near $Da_{E,R}$ are identified by the linear stability analysis. In 2-D simulations using the perturbed IC, it is found that near $Da_{E,R}$, the flame instability is categorized into four different regimes with different instability characteristics. When the radiation effect is extremely large, decaying or growing oscillatory instability appears although the stretch rate is high enough, and the cellular instability occurs in the whole $Da$ at which the flame can survive.

## 1 Introduction

In general, flame instability should be avoided because it is harmful to combustion systems. The cellular instability, however, has been extensively studied due to the needs of its comprehensive understanding and attractive features. The cellular instability is often observed near extinction limit when the effective Lewis number of premixed flames is less than unity.

The extinction phenomena of nonpremixed flames have been investigated by experiments and numerical simulations with various configurations [1-7]. Recently, when the Lewis number is less than unity, the diffusive-thermal (D-T) instability of opposed nonpremixed tubular flames near extinction was investigated using high fidelity numerical simulation with the linear stability analysis [6]. The experiments were compared with 2-D numerical simulations including multicomponent transport and detailed chemical kinetics, and these showed good agreement [7]. In addition, there have been several studies to identify the instability of nonadiabatic flames with radiative heat loss. In a stagnant mixing layer with unity Lewis number, three types of flame evolution, the decaying, diverging and stable limit-cycle solution, were investigated [8]. The structure and dynamic response of nonadiabatic counterflow flames with nonunity Lewis number were identified by 1-D/2-D simulations employing different initial conditions [9].

In the present study, therefore, high fidelity numerical simulations using various initial conditions based on the linear stability analysis are performed to obtain a comprehensive understanding of cellular and oscillatory instabilities of opposed nonpremixed tubular flames near radiation-induced extinction limit.

## 2 Problem Formulation

To obtain extinction information, 1-D analysis is conducted. As in refs [5, 6, 8, 9], the governing equation including radiative heat loss is formulated as follows:

$$u_r \frac{d}{dr}\begin{pmatrix} T \\ Y_F \\ Y_O \end{pmatrix} = \frac{1}{r}\frac{d}{dr}\left(r\frac{d}{dr}\right)\begin{pmatrix} T \\ Y_F/Le_F \\ Y_O/Le_O \end{pmatrix} + Da Y_F Y_O e^{-T_a/T}\begin{pmatrix} q \\ -\alpha_F \tilde{Y}_{O,2} \\ -\alpha_O \tilde{Y}_{F,1} \end{pmatrix} - I \times Da \begin{pmatrix} T^4 - {T_\infty}^4 \\ 0 \\ 0 \end{pmatrix}, \quad (1)$$

where $T$, $Y_F$, and $Y_o$ are the non-dimensional temperature, fuel and oxidizer mass fractions, respectively. To investigate the effects of radiative heat loss, the radiative heat loss term, $I \times Da(T^4 - T_\infty^4)$, is considered in the energy equation of Eq. (1). The $I$ denotes the intensity of radiation, and it is an important nondimensional parameter to show the ratio the radiative heat of transfer thermal energy production. In the present study, the radiation intensity was controlled by using different $I$ values. For the details of parameters and boundary conditions, readers are referred to [6].

The maximum temperature, $T_{max}$, as functions of $Da$ with four different $I$, is shown in Fig. 1. These isolas are obtained by solving Eq. (1) using the Newton-Raphson method with a simple continuation algorithm. The upper branch of isolas is well-burning state and the lower branch represents unstable and physically unrealistic. Figure 1 shows that two extinction Damköhler numbers, $Da_{E,R}$ and $Da_{E,S}$, are obtained. The flammable region decreases as $I$ increases. It is noted that for relatively-large $I = 3.76\times10^{-7}$, $Da_{E,S}$ comes close to $Da_{E,R}$, which implies that for this case, the radiation effect cannot be ignored even near high stretch-induced extinction. In the present study, $I = 10^{-8}$ for which the effects of radiation can be ignored near $Da_{E,S}$ is adopted to see the ordinary phenomena. In addition to that, the results of extremely high radiative intensity, $I = 3.76\times10^{-7}$, is only covered in Section 3.3.

* Corresponding author. Fax: +82-52-217-2449
E-mail address: csyoo@unist.ac.kr

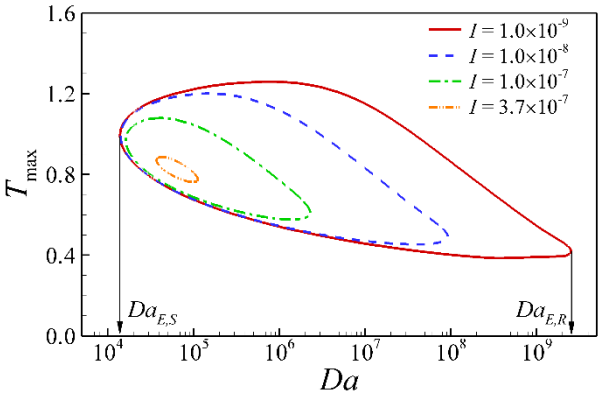


Figure 1: The maximum temperature, $T_{max}$, as functions of Damköhler number, $Da$, with different radiative intensity, $I$.

## 3 Results and Discussion

### 3.1 Linear stability analysis

The linear stability analysis helps to predict flame instability characteristics with good agreement [6]. However, the stability analysis near $Da_{E,R}$ is uncommon. In the analysis, the solution variables, $T$, $Y_F$, and $Y_O$, are defined by the sum of the steady solution of the 1-D tubular flame, denoted by an overbar, and small harmonic perturbations:

$$T = \bar{T}(r) + \epsilon T'(r)e^{ik\theta+\lambda t}, Y_F = \bar{Y}_F(r) + \epsilon Y_F'(r)e^{ik\theta+\lambda t},$$
$$Y_O = \bar{Y}_O(r) + \epsilon Y_O'(r)e^{ik\theta+\lambda t} \quad (2)$$

where $\lambda$ is a complex number whose the real part, $\lambda_R$, represents the growth rate, $k$ is the wavenumber, and $\epsilon$ is the small perturbation amplitude. Substituting Eq. (2) into Eq. (1) and linearizing the equation, an eigenvalue problem of $(\mathbf{A} - \lambda\mathbf{B})\mathbf{x}' = 0$ is then obtained by discretizing, where $\mathbf{x}'$ is the discretized solution vector including $T'$, $Y_F'$, and $Y_O'$. The eigenvalues, $\lambda = \lambda_I i + \lambda_R$, of perturbed governing equations play an important role to identify flame instability, because if $\lambda_R$ is large enough to have an effect to the solution, then the instability can occur. If $\lambda_I$ is zero, the non- or cellular instability depends on the sign of $\lambda_R$. Similarly, if $\lambda_I$ is nonzero, the growing or decaying oscillatory instability rests on whether $\lambda_R$ is positive or negative. In addition, the cell number is related by the wavenumber, $k_{max}$, at which attains its maximum value for a given $Da$. Therefore, prior to conducting 2-D simulations, the linear stability analysis is conducted to find the critical Damköhler numbers which can distinguish the cellular and oscillatory instabilities.

The largest growth rate, $\lambda_R$, as functions of wavenumber, $k$, and Damköhler number, $Da$, is as shown in Fig. 2. The graph gradually moves upward with increasing $Da$, and finally $\lambda_R$ at $k = 0$ has positive value (Fig. 2c). Two critical Damköhler numbers are obtained: thresholds of cellular instability, $Da_{C,C} = 5.76\times10^7$ (Fig. 2a), and growing oscillatory instability, $Da_{C,O} = 6.17\times10^7$ (Fig. 2b). Therefore, it may be conjectured that the cellular instability occurs if $Da$ is larger than $Da_{C,C}$, and the growing oscillatory instability first appears at $Da_{C,O}$.

The wavenumber, $k_{max}$, decreases gradually from 28.8 at $Da_{C,C}$ with increasing $Da$, and $\lambda_R$ also increases at $k_{max}$. As mentioned above, $k_{max}$ is related to the cell number. Therefore, it can be expected that the cell number decreases as $Da$ increases. The impact of oscillation also reduces the time for the occurrence of the D-T instability, because the region of positive $\lambda_R$ increases.

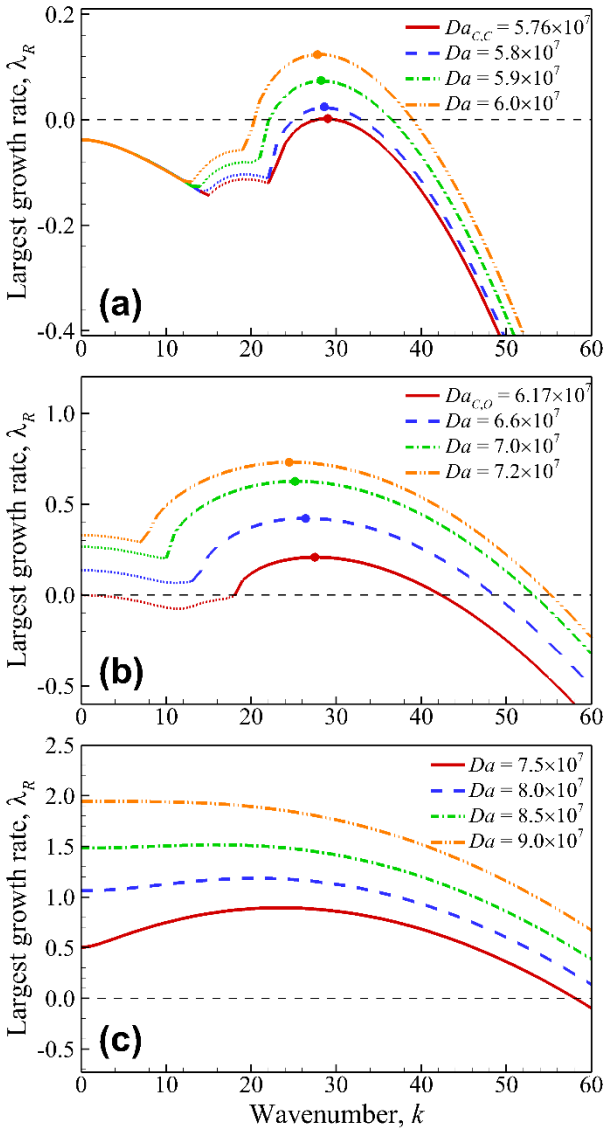


Figure 2: The largest growth rate, $\lambda_R$, as functions of wavenumber, $k$, for different Damköhler numbers, $Da$s. Dotted segments mean the imaginary part of $\lambda \neq 0$.

### 3.2 Effects of small amplitude disturbance

The fundamental characteristics of nonpremixed tubular flames are obtained using the perturbed initial condition (IC) with a fixed $Da$. The perturbed IC is initialized by a well-burning tubular flame having small ($\sim O(\varepsilon)$) amplitude disturbance from 1-D solutions. The perturbation amplitude, $\varepsilon$, of $10^{-5}$ is selected to make a minimized condition.

The variation of the maximum temperature with numerical time is as shown in Fig. 3. The cellular instability can be identified by a sudden rise of temperature. Once the cellular instability occurs, the maximum temperature does not change anymore in time. Note that the oscillatory instability, therefore, can be observed only during the early stage of simulations. The cellular instability can be distinguished by the $Da_{C,C}$ from the linear stability analysis in Fig. 3a. Likewise, it is verified in Fig. 3b that $Da_{C,O}$ divides into decaying and growing oscillatory instability. The oscillatory characteristics such as the amplitude and duration of the oscillation become prominent as the positive region of $\lambda_R$ increases with increasing $Da$. As a result, the oscillation promotes the occurrence of the cellular instability. In Fig. 3c, the

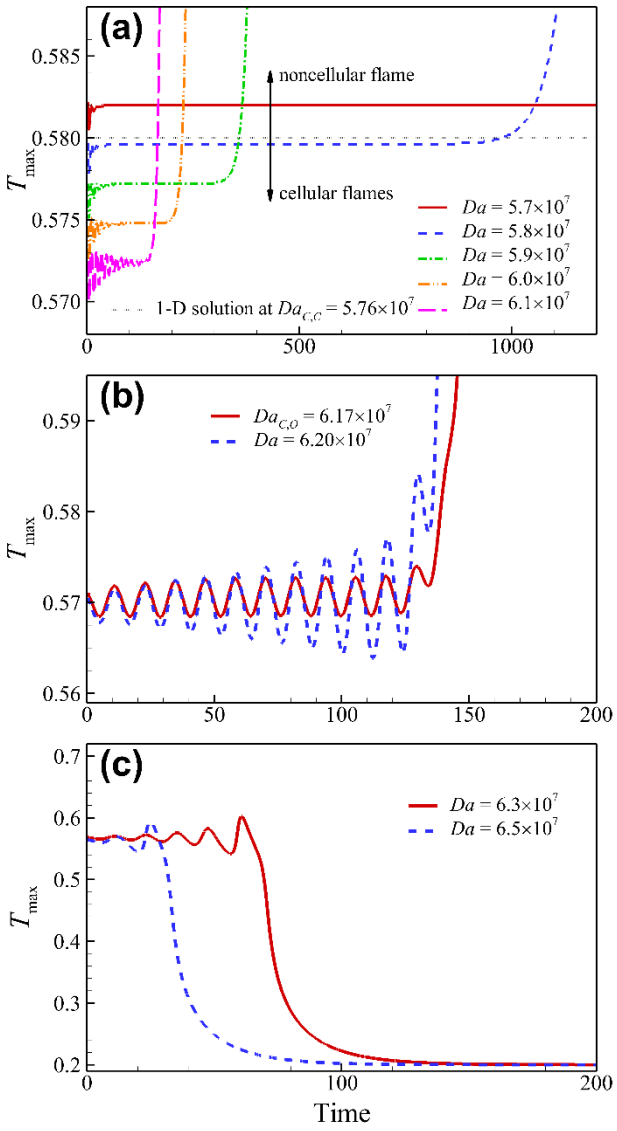


Figure 3: The variation of the maximum temperature, $T_{max}$, with time: (a) the decaying oscillation, (b) the growing oscillation with cellular instability, and (c) the extinction.

flames of which $Da$ is greater than $Da_{C,O}$ cannot sustain from the growing oscillation, and finally are extinguished although the corresponding 1-D solution exists.

The summary of numerical simulations with linear stability analysis near large radiation-induced extinction Damköhler number, $Da_{E,R}$, is shown in Fig. 4. Depending on the instability characteristics, the vicinity of $Da_{E,R}$ is divided into four regimes by two critical $Da$s: $Da_{C,C}$ and $Da_{C,O}$, and $Da_{E,P}$ , which denotes the 2-D extinction $Da$ using the perturbed IC with a fixed $Da$ (=$6.28\times10^7$), as shown in Fig. 4: Regime I. ND ($Da < Da_{C,C}$), Regime II. CD ($Da_{C,C} \leq Da < Da_{C,O}$), Regime III. CG ($Da_{C,O} \leq Da < Da_{E,P}$), and Regime IV. EG ($Da \geq Da_{E,P}$). In first column of table, N, C, and E denote noncellular, cellular, and extinction, respectively. In second column, D and G denote decaying and growing oscillation, respectively. Note that it is reasonable to predict the 2-D simulation outcome wherever the vicinity of $Da_{E,S}$ and $Da_{E,R}$ through a 1-D linear stability analysis with good agreement.

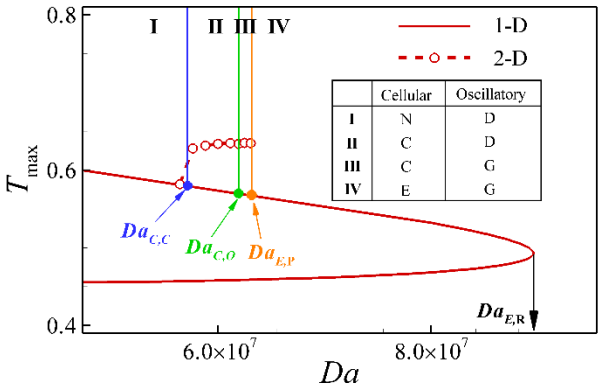


Figure 4: The summary of numerical simulations with linear stability analysis near large radiation-induced extinction Damköhler number, $Da_{E,R}$: **N** (noncellular flame), **C** (Cellular flame), **E** (Extinction), **D** (Decaying), and **G** (Growing)

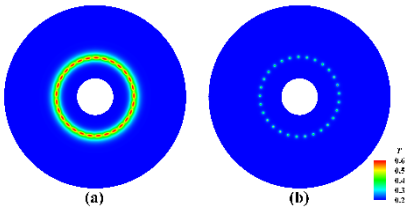


Figure 5: Temperature isocontours using the perturbed IC at (a) $Da = 5.8\times10^7$ and (b) $Da = 1.74\times10^9$.

It is possible to make the cellular flame survive at $Da > Da_{E,R}$, if the $Da$ increases successively with previous solution. To find a global extinction $Da$, 2-D simulations are conducted using the perturbed IC with increasing $Da$ from $Da_{C,C}$ gradually. Figure 5 shows the temperature isocontours of initial flame at $Da$ $5.80\times10^7$ and (b) the cellular flame closed to global extinction $Da = 1.74\times10^9$, respectively. Decreasing each cell size as shown in Fig. 5, the maximum temperature does not change until $Da = 10^9$ due to the balance between radiative heat loss and reaction by high $Da$. However, the flame temperature decreases as $Da$ increases till the global extinction $Da$, $1.74\times10^9$.

### 3.3 Effects of extremely high radiative intensity

| $Da$[a] | $k_{max}$[b] | $N_{cell}$[c] | Sign[d] | Oscillation[e] |
|---|---|---|---|---|
| 38000 | 10.0 | E | + | G |
| 38732 | 10.1 | 10 | + | G |
| 50000 | 10.8 | 11 | - | D |
| 60000 | 11.2 | 11 | - | D |
| 70000 | 11.6 | 12 | - | D |
| 80000 | 11.8 | 12 | - | D |
| 88600 | 11.9 | 12 | + | G |
| 90000 | 11.9 | 11 | + | G |
| 100000 | 11.8 | E | + | G |

a. Damköhler number, two extinction $Da$s are 37363 and 112500, respectively.

b. Wavenumber of the maximum largest growth rate.

c. Cell number, E: extinction.

d. Sign of maximum largest growth rate when the imaginary part, $\lambda_I$, is not equal to 0.

e. Oscillation characteristics, D: decaying; G: growing.

Table 1: Flame instability characteristics for extremely high radiative intensity, $I = 3.7\times10^{-7}$, in overall $Da$ region.

Generally, the D-T instability only occurs near an extinction limit when the Lewis number is less than unity, because the flame cell formation by fuel focusing effect appears to help that the flame sustains from the harsh environment. However, if the intensity of radiation is extremely high, $I = 3.76\times10^{-7}$ in the present study, the possibility which induce the D-T instability is shown in all domain. The flame instability characteristics for extremely large radiative intensity, $I = 3.76\times10^{-7}$, in the entire range of *Da* are written in Table 1. Two extinction *Da*s obtained from 1-D simulations are $Da_{E,S} = 37363$ and $Da_{E,R} = 112500$, respectively. The results near $Da_{E,R}$, do not seem to be special. However, near $Da_{E,S}$, the decaying and growing oscillatory instability are observed, and the tendency is similar to the vicinity of a large radiation-induced extinction. Two $Da_{C,O}$ are observed, no $Da_{C,C}$. It is also noticeable that the nonpremixed tubular flames under extremely high radiation always exist with the cellular instability.

## 4 Conclusions

The flame instability and cell dynamics of nonpremixed tubular flames with radiative heat loss are investigated using 2-D simulations with the linear stability analysis based on 1-D analysis. Two different extinction *Da*s, high stretched-induced and radiation-induced extinction *Da*, are obtained as various intensities of radiation, *I*. The perturbed initial condition is used to elucidate the fundamental instability characteristics near $Da_{E,R}$. In conclusion, the vicinity of $Da_{E,R}$ is divided into four regimes as shown in Fig. 4, Regime I. ND ($Da < Da_{C,C}$), Regime II. CD ($Da_{C,C} \leq Da < Da_{C,O}$), Regime III. CG ($Da_{C,O} \leq Da < Da_{E,P}$), and Regime IV. EG ($Da \geq Da_{E,P}$), and these can be predicted by the linear stability analysis with good agreement. The global extinction *Da* is extended by the cellular instability. If radiative heat loss is relatively too large, $I = 3.76\times10^{-7}$, the radiation effects cannot be ignored near high stretched nonpremixed tubular flames, since the oscillatory instability is observed. In the specific condition, the cellular instability appears in overall *Da*.

## 5 Acknowledgment

This work was supported by the Space Core Technology Development Program (No.2015M1A3A3A02027319) and Basic Science Research Program (No.2015R1A2A2A01007378) through the National Research Foundation of Korea grant funded by the Ministry of Science, ICT and Future Planning.

## References

[1] M. Short, J. Buckmaster, S. Kochevets, Combust. Flame 125 (2001) 893-905.

[2] S. Hu, P. Wang, R. W. Pitz, Proc. Combust. Inst. 31 (2007) 989-996.

[3] S. Hu, R. W. Pitz, Combust. Flame 156 (2009) 51-61.

[4] S. Hu, R. W. Pitz, Y. Wang, Combust. Flame 156 (2009) 90-98.

[5] S. W. Shopoff, P. Wang, R. W. Pitz, Combust. Flame 158 (2011) 876-884.

[6] H. S. Bak, S. R. Lee, J. H. Chen, C. S. Yoo, Combust. Flame 162 (2015) 4612-4621.

[7] C. A. Hall, R. W. Pitz, Combust. Flame 36 (2017) 1595-1602.

[8] C. H. Sohn, J. S. Kim, S. H. Chung, K. Maruta, Combust. Flame 123 (2000) 95-106.

[9] J. R. Nanduri, C. J. Sung, J. S. T'len, Combust. Theory Model. 9 (2005) 515-548.